AIAA JOURNAL
Vol. 41, No. 12, December 2003

Influence of Orifice Orientation on a Synthetic Jet–Boundary-Layer Interaction

Amanda Bridges* and Douglas R. Smith†
University of Wyoming, Laramie, Wyoming 82071-3295

The mean streamwise velocity field downstream of a synthetic jet embedded in a turbulent boundary layer (Re_θ = 830) was investigated experimentally. Of particular interest was the change in the mean flowfield resulting from changes in the yaw orientation of the rectangular synthetic jet orifice. Three yaw angles (β = 0, 10, 20 deg) were considered. Time-averaged and phase-averaged hot-wire measurements were obtained at two positions downstream of the synthetic jet actuator. The measurements show that when the orifice is aligned with the mean freestream velocity (β = 0 deg), a flow structure consistent with a weak counter-rotating vortex pair was observed in the boundary layer. For β = 10 deg, the mean streamwise velocity contours suggest the presence of a single vortex in the boundary layer, whereas for β = 20 deg, the flow structure resembles a horseshoe vortex formed as a result of flow blockage by the jet.

I. Introduction

PERHAPS one of the more notable advances to have occurred in flow control technology in the past 15 years is the application of surface-issuing jets for separation control on aerodynamic surfaces. The concept was introduced by Johnston and Nishi,[1] who proposed using circular jets, skewed and inclined to the wall, to generate streamwise vortices for the purpose of mitigating boundary-layer separation. The skew and inclination angles have subsequently been shown to affect the strength and sign of the ensuing vortices[2] and the control effectiveness of the jet. If the jet orifice is noncircular, then, in addition to skew and inclination, the yaw angle of the major axis of the orifice can influence the flow control effectiveness of the jet.[3]

Early work with flow control jets all used a steady rate of mass injection until Seifert et al.[4] revealed that an unsteady blowing jet could be as effective at separation control as a steady jet but with less mass flow. More recent work suggests that perhaps the most efficient jet control effect comes from a synthetic (oscillatory) jet where the time-averaged mass flux through the orifice is zero, but the net momentum is nonzero. The control effectiveness of synthetic jets has been demonstrated for several internal and external flowfields.[5–7]

Although the control effectiveness of synthetic jet actuators in an application setting has been confirmed through a number of studies, the fluid dynamic mechanism by which control is effected is not well understood. Issues like yaw angle and velocity ratio that have been studied for steady control jets have not been investigated for synthetic jets. Moreover, the role played by the inherently unsteady nature of a synthetic jet in the interaction with the controlled flow is not known. Some recent work by Rinehart and Glezer[8] and Smith[9] suggests that away from the immediate vicinity of the jet orifice the flowfield is steady in the mean and that the interaction of a synthetic jet and a boundary layer creates a secondary flow consisting primarily of streamwise vortices.

To evaluate the efficiency of a synthetic jet for reducing the boundary-layer susceptibility to separation, we must evaluate the role of actuator configuration in the control effect. For example, to mix high-momentum fluid from the edge of the boundary-layer with low-momentum fluid near the wall, a streamwise vortex structure should be of the same scale as the boundary-layer thickness. The streamwise vortices originating from the interaction between a synthetic jet actuator and a crossflow boundary layer would be expected to have a size that is initially determined by the penetration depth of the jet. For a rectangular steady jet, Weston and Thames[10] have shown that the penetration depth will depend on the orientation, or yaw, of the major axis of the orifice relative to the mean cross-stream velocity direction. Perhaps of equal importance in determining the penetration depth and ensuing flow structure is the velocity ratio (jet to freestream) and duty cycle. For steady jets issuing into a crossflow, the penetration depth has been shown to scale directly with the velocity ratio.[11] If the jet is pulsed, there exists a range of frequencies where the penetration is also frequency dependent and duty cycle dependent.[12,13] Pulsed jets at low frequencies with short injection times (and short duty cycles) penetrate deeper into the crossflow.[14]

To improve the implementation of synthetic jet actuators in flows requiring active control, a better understanding of the character and structure of the interaction between the jet and the embedding boundary layer is required. In this study, we sought to isolate and identify the role of orifice orientation (yaw angle) on synthetic jet flow control effectiveness. Time-averaged and phase-locked measurements were used to build a data set of boundary-layer profiles with high spatial resolution in the cross-span and cross-stream directions. Using this data set, we examine the near-field behavior of the interaction, look for the appearance of streamwise-aligned vortices, and try to understand to what degree yaw angle affects the origin and formation of these vortices.

II. Experimental Approach

The experiments were performed in the low-speed wind tunnel at the University of Wyoming Aerodynamics Laboratory. The boundary-layer flow was developed on a flat plate mounted parallel to the test-section floor. The leading edge of the plate was a 4:1 ellipse, and transition occurred naturally near the leading edge of the plate. The plate was adjusted to have a zero pressure gradient along the length and uniform pressure across the width. Measurements of the surface pressure coefficient (C_p) varied by less than 1% along the length of the plate.

The synthetic jet actuator was a resonating-cavity device driven with two 50-mm-diam piezoelectric disks mounted on opposite sides of the actuator cavity. The orifice of the actuator was rectangular with dimensions 50 (L) by 0.51 mm (h). The depth of the orifice was 2.4 mm. The resonant, and subsequent operating, frequency of the

Received 20 January 2003; revision received 12 May 2003; accepted for publication 21 May 2003.

*Graduate Research Assistant, Department of Mechanical Engineering, P.O. Box 3295. Student Member AIAA.
†Assistant Professor, Department of Mechanical Engineering, P.O. Box 3295. Senior Member AIAA.

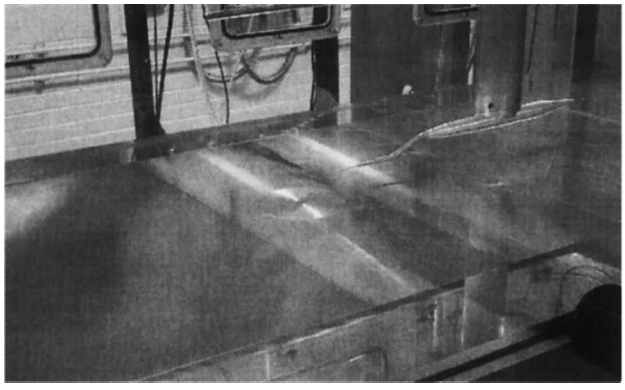

a)

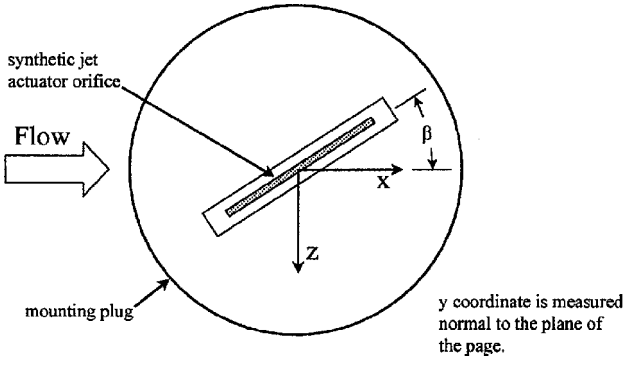

b)

Fig. 1 Experimental setup: a) photograph of the synthetic jet actuator and mounting plug in the test surface; b) close-up sketch of the synthetic jet actuator and mounting plug.

actuator was found experimentally to be 500 Hz. The actuator was mounted in a circular plug, and the plug was installed flush with the surface of the flat plate. A retaining ring secured the plug in the plate and allowed the plug to be rotated continuously through 360 deg (Fig. 1). The yaw angle of the orifice, β, corresponded to the angle the major axis of the orifice made with the freestream direction; that is, for $\beta = 0$ deg the orifice axis and freestream velocity vector were parallel. Positive values of β were measured counterclockwise when the actuator is viewed from above (Fig. 1b). Three values of β were investigated: 0, 10, and 20 deg.

All boundary-layer measurements were obtained with a nominal freestream velocity of 17.0 ± 0.5 m/s. For all test cases, the boundary layer upstream of the actuator was turbulent. Figure 2 shows profiles of the mean and fluctuating components of the streamwise velocity in the upstream boundary layer. The boundary-layer thickness δ_o at a position immediately upstream of the actuator plug was 9.7 ± 0.3 mm. A reference coordinate system was located at the center of the actuator orifice with x in the streamwise direction, z in the cross-span direction, and y measured normal to the wall (Fig. 1b). Because the edge of the boundary layer may be obscured by the synthetic jet interaction, all figures presented show the distance from the wall, y, scaled by the upstream boundary-layer thickness δ_o. The cross-span distance z is shown in dimensional coordinates (mm) to facilitate comparisons between the three yaw-angle cases.

Mean and fluctuating velocity measurements were acquired using a single normal-sensor hot-wire. The hot-wire probes were miniature-sensor boundary-layer probes. The wire was 5 μm in diameter with a 1.2-mm active length. Static hot-wire calibrations were performed in situ using a King's law fit. The freestream flow temperature was recorded both during the calibration and during the boundary-layer surveys. To account for flow temperature drift during a survey, all hot-wire voltages were corrected to a reference temperature.

The mean and fluctuating hot-wire signals were measured independently after low-pass (10 Hz) and bandpass (10 Hz–4 kHz) filtering, respectively. At each point in a boundary-layer survey, 96,000 data points were obtained at a sampling rate of 10 kHz. In the data acquisition, the actuator driver signal was also recorded to permit phase-locked analysis of the hot-wire signal. With a data sampling rate of 10 kHz and an actuator driver frequency of 500 Hz, 20 profiles, equally spaced throughout the driver period, were obtained. For each point in a boundary-layer profile, a linear interpolation scheme was used to shift the phase-averaged data to the same relative times in the actuator driver period.

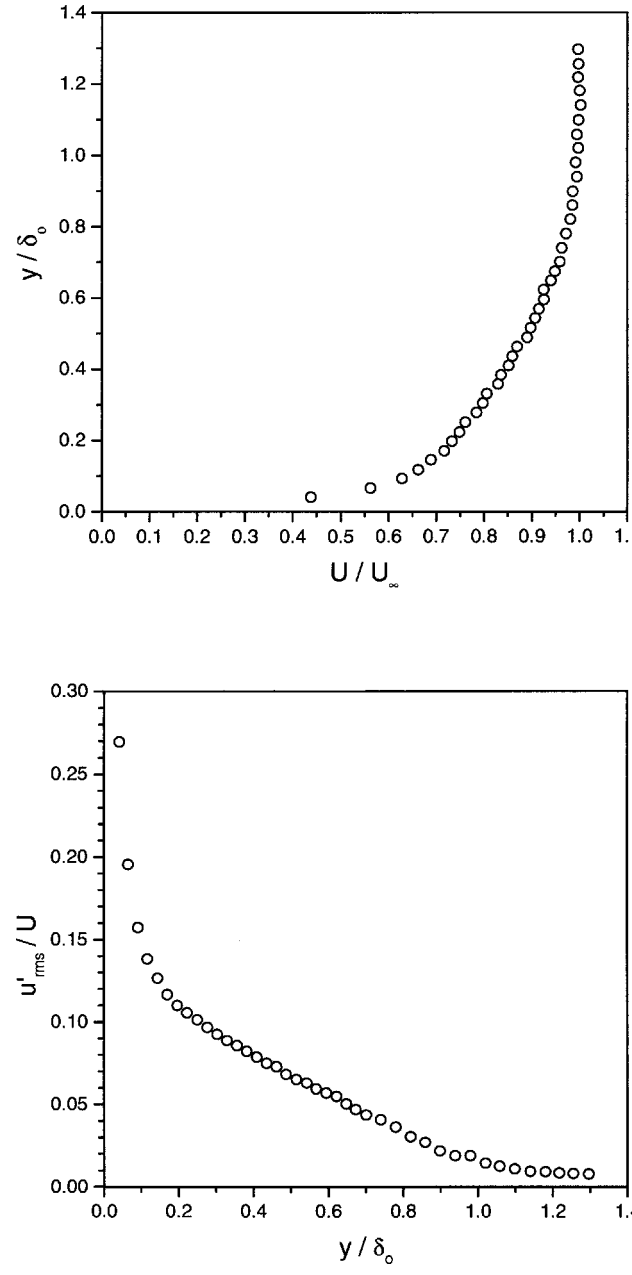

Fig. 2 Profiles of the mean (top) and the rms fluctuating (bottom) components of the streamwise velocity in the upstream boundary layer.

For each yaw angle β, profiles of the instantaneous velocity in the boundary layer were measured at two positions downstream of the actuator. At each streamwise position, the boundary-layer profiles were obtained at multiple cross-span positions that extended from the wind-tunnel centerline to the edge of the jet–boundary-layer interaction on either side.

The synthetic jet actuator performance was tested in a quiescent environment prior to installation in the wind-tunnel test. The actuator was calibrated by recording the velocity signal $u(t)$ from a hot-wire placed in the plane of the orifice along the orifice centerline.

The outstroke portion of this velocity trace was identified and used to estimate a velocity U_o defined as L/τ, where L is the effective stroke length of the actuator and τ is one-half the period of the actuator forcing signal.[15] In these experiments, U_o was estimated to be 14 m/s, and to permit comparisons with studies involving a steady jet in a crossflow, a velocity ratio r was defined as

$$r = \left(\frac{\rho_j U_o^2}{\rho_\infty U_\infty^2}\right)^{\frac{1}{2}} = \frac{U_o}{U_\infty}$$

In the current set of experiments, we estimated r to be 0.82. Note that in previous studies of rectangular vortex generator jets, a value of r near unity was concluded as optimal for the formation of a single streamwise vortex within the boundary layer.[3] Due to constraints imposed by the synthetic jet actuator, a value of $r = 0.82$ was as close to unity as possible in the current experiment. Nevertheless, this velocity ratio is representative of a typical value for a boundary-layer flow control application.

III. Results and Discussion

Using the aforementioned techniques, this study explored the influence of orifice yaw angle on the mean boundary-layer structure downstream of a rectangular synthetic jet. Based on preliminary observations three yaw angles were chosen for study: 0, 10, and 20 deg. In the preliminary experiments (not discussed here), we discovered that with the current velocity ratio ($r = 0.82$) a yaw angle greater than 20 deg produced a very weak interaction that was confined to a narrow region near the wall and inaccessible to the current hot-wire probe measurements.

Note that a single, normal hot-wire is insensitive to flow direction. In this experiment, velocities normal to the wall tended to increase the apparent streamwise velocity, and cross-span velocities had the opposite effect. Measurements by Zhang and Collins[3] with laser Doppler anemometry in the boundary layer downstream of a steady rectangular jet with velocity ratio of 1.0 showed velocities in the y–z plane that were at most 10% of the mean freestream velocity. This suggests that while there certainly is some corruption of the velocity measurements by wall-normal and cross-span velocities, the hot-wire is primarily measuring the streamwise component of the velocity.

A. Time-Averaged Velocity Contours

Figure 3 shows contours of the mean streamwise velocity at two streamwise locations, $x/L = 1.0$ and 1.45, for $\beta = 0$ deg. In this and all subsequent figures the abscissa is shown in dimensional coordinates to facilitate a comparison of the interaction scale for different β. The presence of the jet in the boundary layer is quite evident from these contours and manifests as a region of reduced velocity, almost circular in shape, centered near $y/\delta_o = 0.8$ and extending beyond the edge of the boundary layer. At the upstream position, the effect of the jet on the boundary-layer flow near the wall does not appear to be large, but farther downstream, as the jet interaction grows in the vertical and cross-span directions, we observe regions of high-momentum fluid pushed down in the boundary layer to either side of the jet. Immediately beneath the jet, however, the velocity appears mostly unchanged in magnitude from the contours in the regions outside of the interaction. Interestingly, the minimum in the velocity defect does not appear to move away from the wall between $x/L = 1.0$ and 1.45, yet the top of the defect has moved into the freestream by more than $0.2\delta_o$ over the same streamwise distance. The velocity minimum in the defect is decreasing presumably as turbulence mixes higher momentum fluid from the surroundings into this region.

Of particular note in these contours is the rapid change in spanwise scale of the interaction, which at $x/L = 1.0$ is approximately 10 mm. An appreciation for this change can be obtained by first noting that the orifice width h is 0.51 mm. Next, if, during the formation phase, the jet has a width of $5h$ (see Ref. 15), then as the jet interacts with

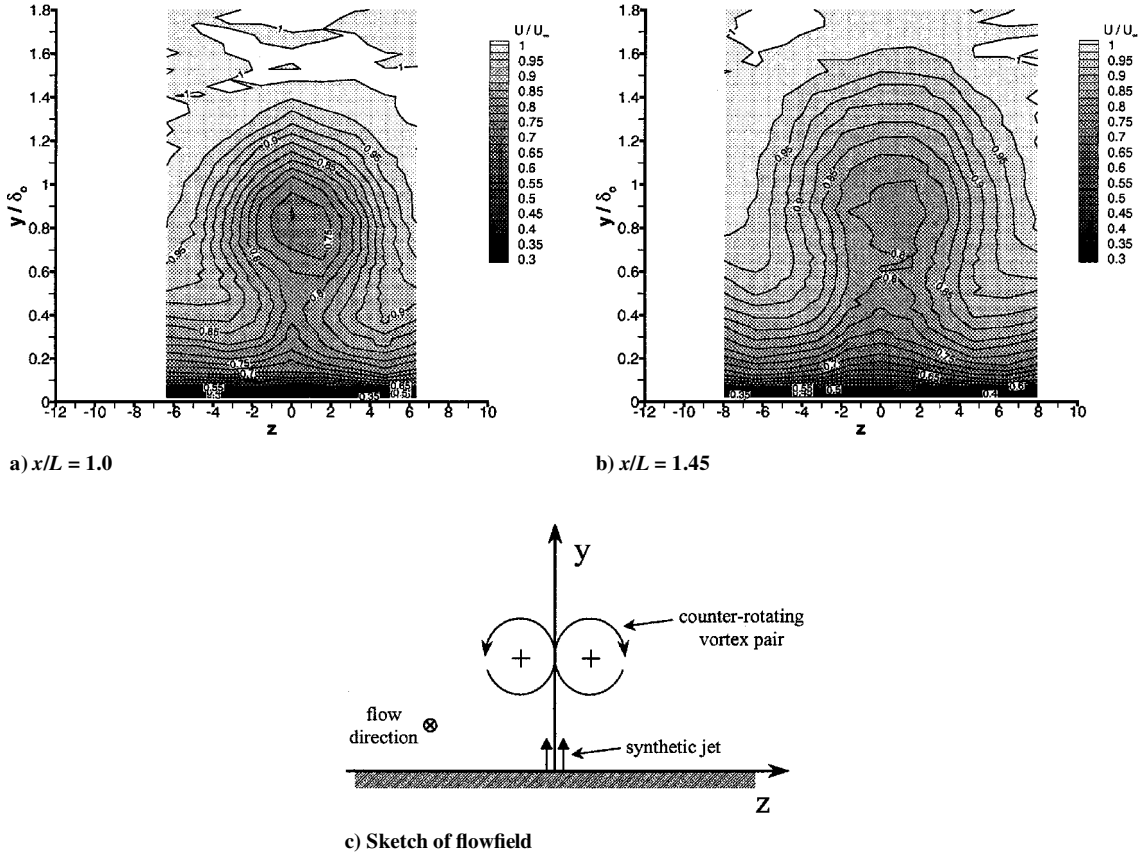

a) $x/L = 1.0$

b) $x/L = 1.45$

c) Sketch of flowfield

Fig. 3 Comparison of the mean streamwise velocity contours at two streamwise locations for $\beta = 0$ deg. Also shown is a sketch of the proposed mean flow structure.

the boundary layer, its width increases by a factor of 4 from 2.5 to 10 mm ($\approx 20h$). Furthermore, noting that δ_o/h is approximately 19, the interaction attains a width of approximately one boundary-layer thickness within one orifice length of its inception. The vertical scale may be partially understood by noting that the orifice length L is approximately five times larger than the incoming boundary-layer thickness δ_o, but the height of the interaction is at most $1.5\delta_o$.

The mean velocity contours, particularly at $x/L = 1.45$, suggest that a weak counter-rotating vortex pair may be present in the boundary layer (see Fig. 3c). The rotation of this vortex pair would tend to draw low-momentum fluid up along the centerline of the interaction and push high-momentum fluid down in the boundary layer along the sides of the interaction. The effects are subtle, indicating the vortex pair is likely weak but persistent with the streamwise direction. Moreover, the velocity contours do not exhibit the kidney shape typically observed in a steady jet in a crossflow where the counter-rotating vortex pair is quite evident.

Figure 4 shows contours of the streamwise turbulence intensity, $u'_{\rm rms}/U$, at $x/L = 1.0$ and 1.45 for $\beta = 0$ deg. The shape of these contours is more elliptic, or kidney-shaped, in nature than the mean velocity contours. The size of the interaction appears broader and taller in these contours, but this apparent effect is due to the modulation of the mean flow at the actuator frequency rather than turbulent fluctuations. It is interesting to note here that at both streamwise positions the peak in the turbulence intensity associated with the jet occurs farther from the wall than the minimum in the velocity contours and also moves away from the wall with streamwise distance while the mean defect region remains at the same height. Near the wall, the approximately level contours suggest that the turbulence intensity is unmodified from the boundary layers to either side.

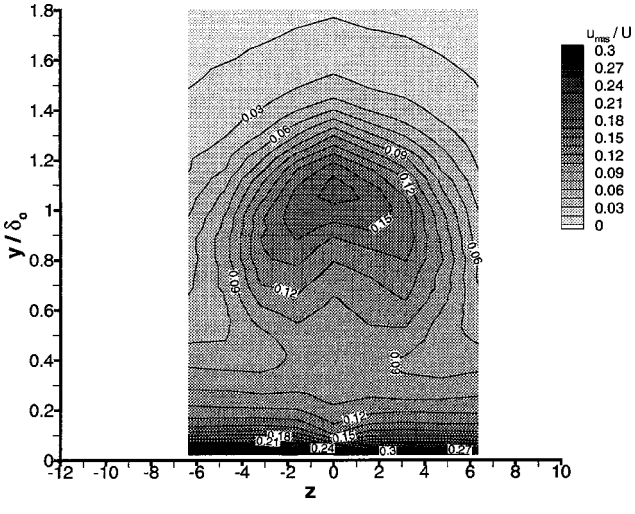

a) x/L = 1.0

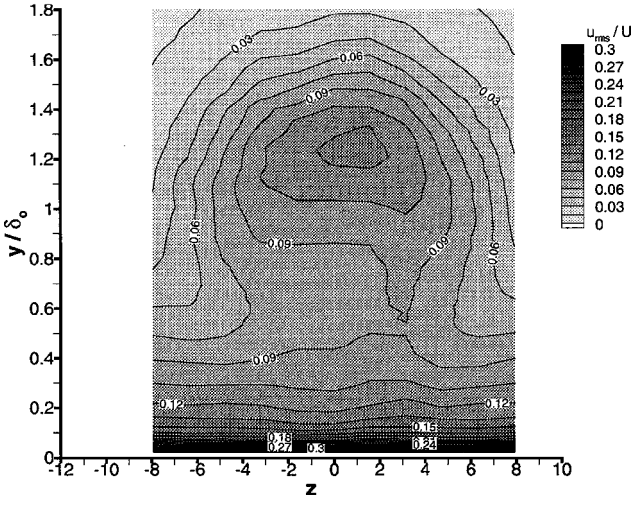

b) x/L = 1.45

Fig. 4 Contours of the streamwise turbulence intensity for β = 0 deg.

For $\beta = 10$ deg, the actuator is no longer symmetrically oriented about the x–y plane. In rotating the orifice through 10 deg, the cross-span length of the orifice, as seen by the incoming flow, increased to approximately 8.7 mm from a value of 0.51 mm when $\beta = 0$ deg. The leading edge of the orifice was displaced to $z = +4.4$ mm, and the trailing edge was displaced to $z = -4.4$ mm.

Figure 5 shows contours of the streamwise velocity at $x/L = 1.0$ and 1.46 for $\beta = 10$ deg. The first point to note in these profiles is that, in comparison with $\beta = 0$ deg, the height to which the interaction rises in the boundary layer is considerably reduced, confined now to the lower 60% of the boundary layer (Fig. 5). This effect is clearly due to the broader initial cross section of the jet. Next, and as expected, an asymmetry appears with respect to the interaction centerline ($z = 0$). A region of velocity defect is observed near $z = 2$ mm and is confined primarily to $z > 0$. For $z < -2$ mm, the contours suggest a fuller velocity profile near the wall. For $x/L = 1.46$, a similar behavior is observed, but with larger spanwise and vertical scales. In particular, we note a region of higher near-wall momentum between $z = -2$ and -7 mm.

Although there may be more than one interpretation for the contour shapes observed here, we propose that in this case they are the result of a single streamwise-aligned vortex arising from the synthetic jet–boundary-layer interaction (see Fig. 5c). To support this conclusion, we compared the velocity contours obtained here with the measurements shown in three prior studies: Shabaka et al.,[16] who studied a single vortex embedded in a turbulent boundary layer; Zhang and Collins,[3] who studied the interaction of a boundary layer with a steady rectangular jet; and Khan and Johnston,[17] who studied the interaction of a boundary layer with a skewed and inclined circular jet. In the latter two studies, the velocity measurements showed very clearly the existence of a single streamwise vortex in the lee of the interaction. By comparison with these previous studies, the mean velocity contours here (Fig. 5) suggest the presence of a vortex with a similar sense of rotation (counterclockwise when looking downstream at the vortex). A vortex of this sense would lead to a downdraft of high-momentum fluid for $z < 0$ and an updraft of low-momentum fluid for $z > 0$. The agreement between the contours shown in Fig. 5a and the contours shown in Fig. 5 of Ref. 17 is particularly striking and provides compelling evidence for the proposed flowfield.

To understand the direction of rotation of the vortex, the synthetic jet must behave not only like a skewed jet in a crossflow but also as an inclined jet in a crossflow. This interpretation is not inconsistent with the observations of Smith et al.[18] for the formation of synthetic jets from adjacent orifices. Smith et al. showed that the synthetic jet formed by the interaction of two adjacent synthetic jets can be turned to either side depending on the relative phases of the jet formation cycles. The turning was the result of a distortion of the jet formation vortices due to the phase difference. In this case, the approach flow distorts the jet formation vortices and does so in such a way as to lead to a downstream turning of the synthetic jet.

Figure 6 shows contours of the streamwise turbulence intensity, $u'_{\rm rms}/U$, at $x/L = 1.46$ for $\beta = 10$ deg. The shapes of these contours support the conclusion of a secondary flow pattern redistributing turbulent fluid within the boundary layer. That is, low-momentum fluid, with high turbulence levels, is swept away from the wall, and high-momentum fluid, with low turbulence levels, is drawn toward the wall.

For $\beta = 20$ deg, the projected area of the jet was approximately 17 mm, with the leading edge of the orifice at $z = +8.5$ mm and the trailing edge at $z = -8.5$ mm. Figure 7 shows contours of the mean streamwise velocity at $x/L = 1.0$ and 1.46 for $\beta = 20$ deg. The presence of the synthetic jet in the boundary layer is much less pronounced in these profiles and is confined to the lower 50% of the boundary layer. For -2 mm $< z < 0$ (Fig. 7), the contours reveal a region of higher momentum near the wall. This region is located closer to the centerline of the interaction than the high-momentum

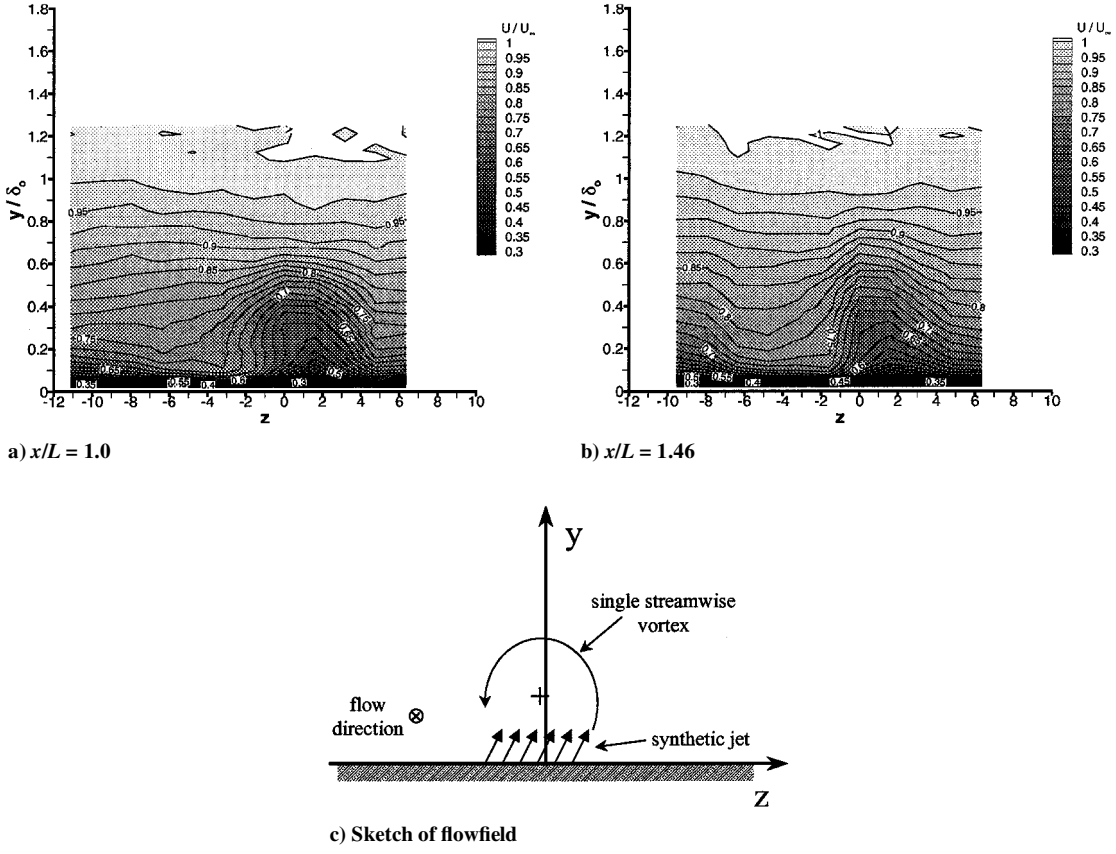

a) $x/L = 1.0$ b) $x/L = 1.46$

c) Sketch of flowfield

Fig. 5 Comparison of the mean streamwise velocity contours at two streamwise locations for $\beta = 10$ deg. Also shown is a sketch of the proposed mean flow structure.

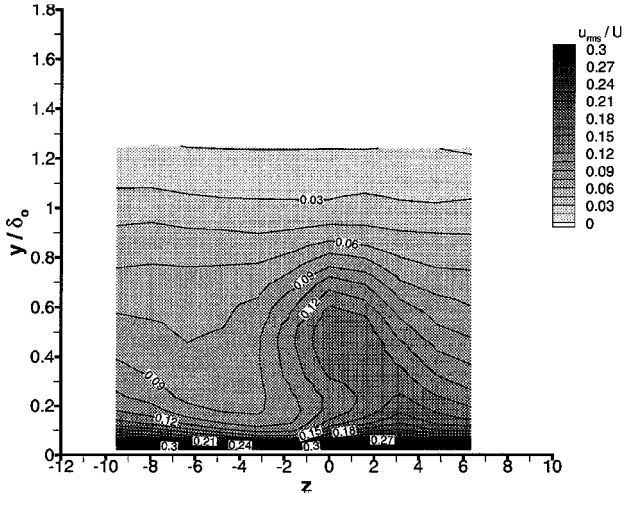

Fig. 6 Contours of the streamwise turbulence intensity for $\beta = 10$ deg: $x/L = 1.46$.

region for $\beta = 10$ deg. For this yaw angle, we propose that the jet acts primarily as an obstruction in the boundary layer and that the high-momentum region near the wall is a consequence of a weak pair of counter-rotating vortices that are, in fact, the legs of a horseshoe vortex formed by the blockage (see Fig. 7c). That the blockage is weak and is modulated at the actuator frequency tends to blur the time-averaged velocity contours; however, the phase-averaged velocity contours, presented in the following section, show more clearly the flowfield structure.

B. Phase-Averaged Velocity Contours

By analyzing the hot-wire signal and the actuator driver signal simultaneously, phase-averaged velocity profiles for the boundary layer were constructed. The angle ϕ is used to denote the phase in the period of the actuator driving signal.

Figure 8 shows phase-locked contours of the streamwise velocity for $\beta = 0$ deg. A sequence of four phase angles in the actuator period (0, 90, 180, and 270 deg) are shown. These contours show very clearly the "pulsing" of the defect region during one actuator cycle. At this streamwise position, the maximum penetration depth of the jet is achieved near the 0-deg phase angle. From 90 to 180 deg, the velocity defect region becomes shallower and shifts down in the boundary layer and is accompanied by a reduction in the vertical scale of the region. Between 180 and 270 deg, the depth of the defect region increases significantly with a steepening of the velocity gradients due to the smaller vertical scale of this region. Finally, in the last quarter of the period, the defect region rises rapidly from below $y/\delta_o = 0.8$ to above $y/\delta_o = 1.1$. Throughout the actuator cycle, the relative shapes of the contours are consistent with the structure proposed from an inspection of the time-averaged contours. This observation suggests that at this location the general features of the boundary-layer structure are established but that the strength, scale, and position are modulated at the actuator frequency.

Figure 9 shows a similar sequence of phase-averaged contours for $\beta = 10$ deg. Unlike the contours at $\beta = 0$ deg, where the flow structure was similar throughout the actuator cycle, these contours show that the flowfield changes quite significantly during the actuator cycle. For $z > 0$, the defect region appearing at $y/\delta_o = 0.3$, and signifying the core of the single vortex, collapses between $\phi = 180$ and 270 deg. This segment of the actuator cycle presumably corresponds to the suction phase when fluid in the boundary layer either flows past the orifice mostly undeflected or into the orifice. During the blowing phase of the actuator cycle (between 0 and 90 deg), the defect region becomes quite pronounced, and the jet contributes to the formation of a single longitudinal vortex. During this segment of the actuator cycle and for $z < 0$, fluid with high streamwise momentum has been swept in toward the wall from higher in the boundary layer.

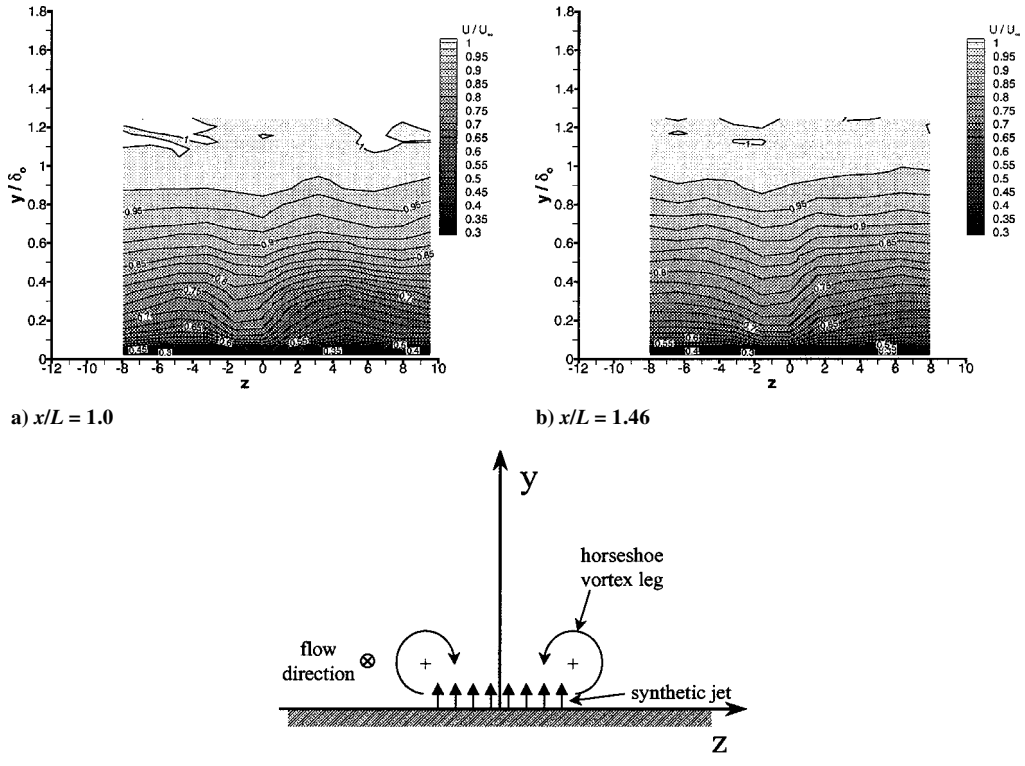

a) $x/L = 1.0$

b) $x/L = 1.46$

c) Sketch of flowfield

Fig. 7 Comparison of the mean streamwise velocity contours at two streamwise locations for $\beta = 20$ deg. Also shown is a sketch of the proposed mean flow structure.

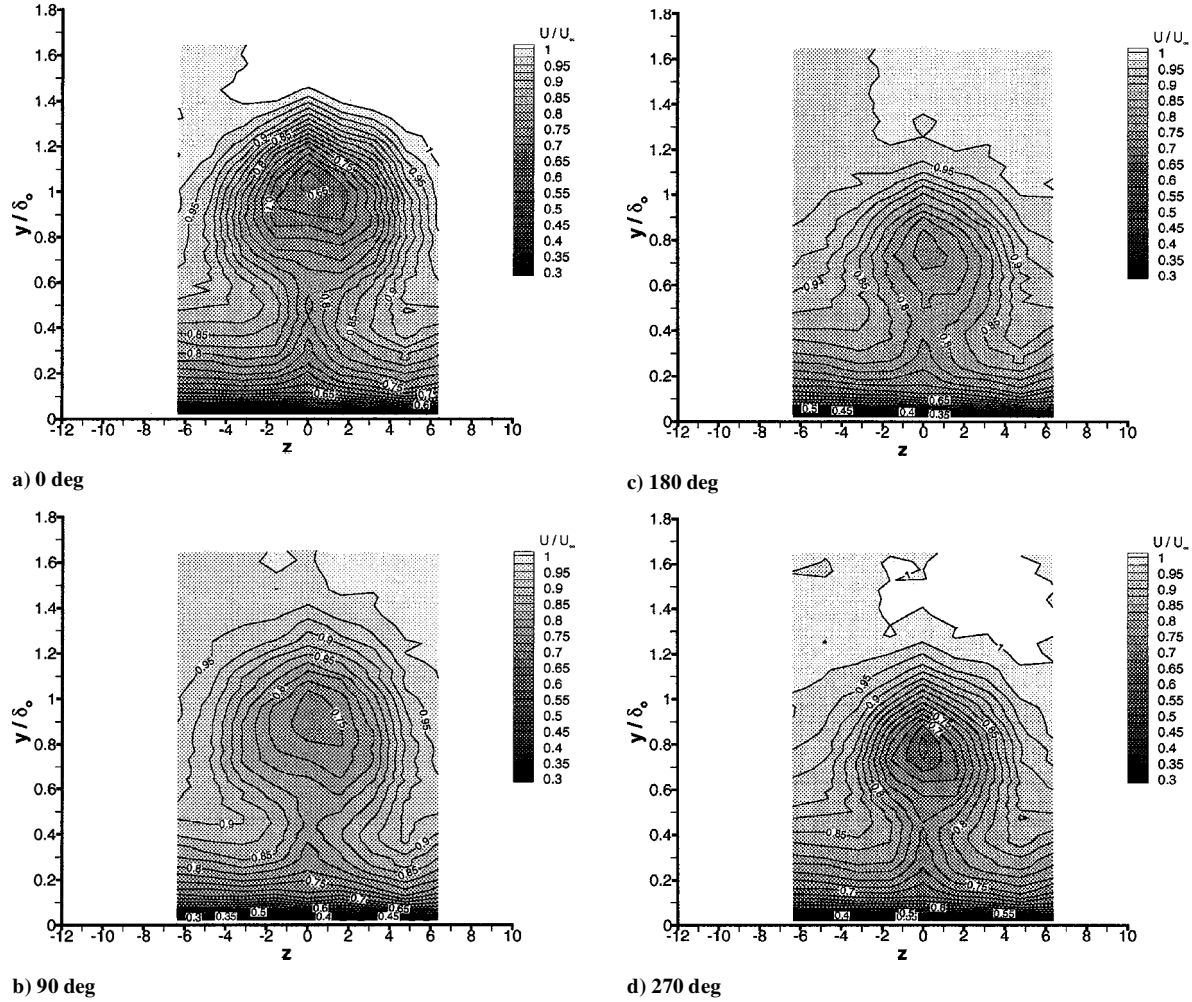

a) 0 deg

c) 180 deg

b) 90 deg

d) 270 deg

Fig. 8 Phase-averaged contours of mean streamwise velocity for $\beta = 0$ deg at $x/L = 1.0$.

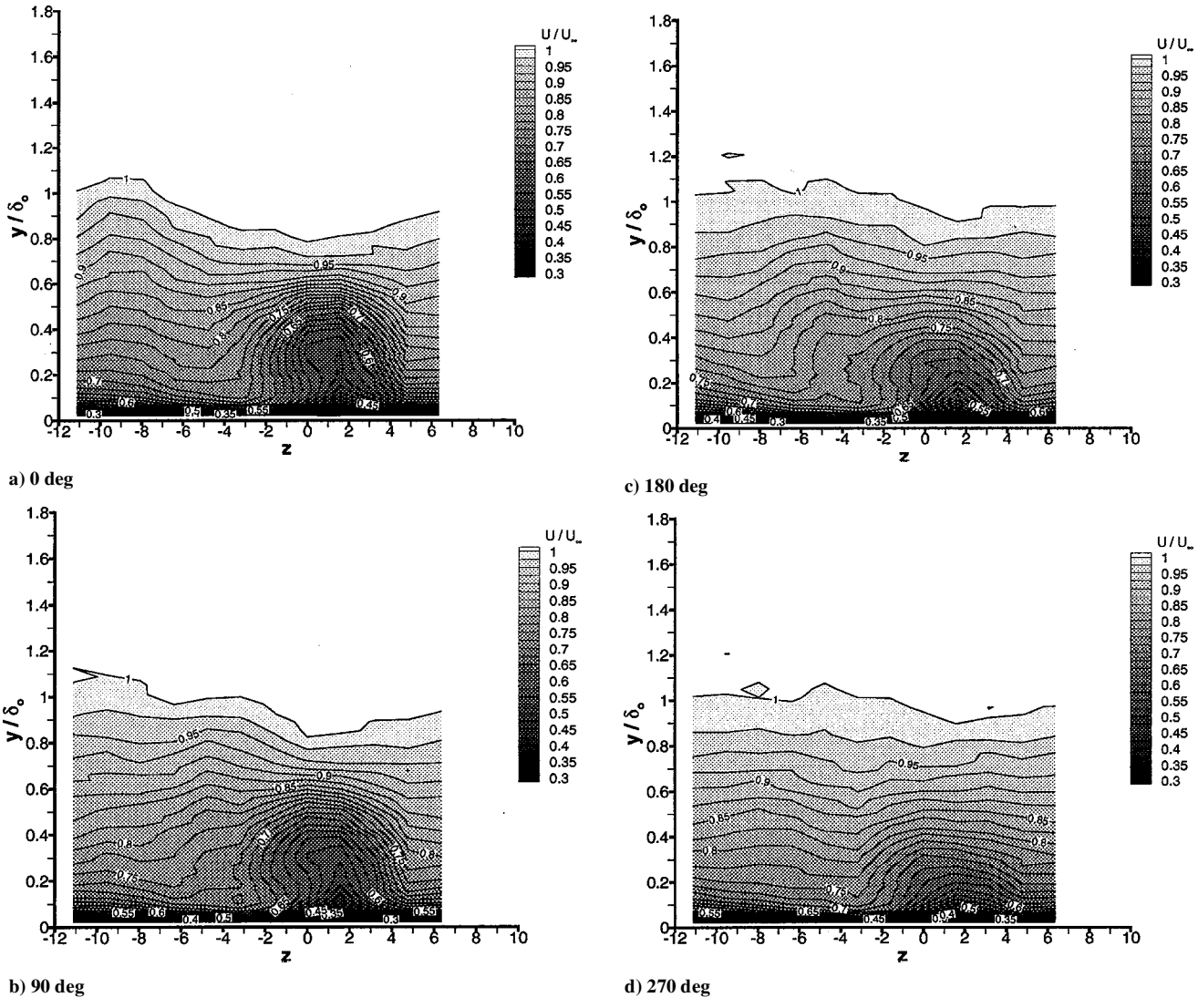

Fig. 9 Phase-averaged contours of the mean streamwise velocity for β = 10 deg at x/L = 1.0.

Finally, the phase-locked contours for $\beta = 20$ deg are shown in Fig. 10. In these figures, we observed a structure that helps elucidate the structure inferred from the time-averaged contours and that appears to evolve from the interaction between the boundary layer and the edges of the jet orifice. This structure is clearly visible for $\phi = 180$ deg at positions of $z = \pm 5$ mm, which lie just inboard of the outer edges of the orifice. From 180 to 0 deg, this structure drifts toward $z < 0$ as it convects downstream and through the measurement plane. The contours at 90 deg indicate that the formation of this interaction begins near this phase in the actuator cycle. The appearance of the interaction, a double-humped low-velocity region to either side of a high-velocity region, suggests that the interaction resembles the horseshoe vortex that forms around an obstacle placed in a boundary layer. Here, of course, the obstacle is the blowing jet that appears periodically at the actuator driving frequency.

C. Effect of Orifice Yaw

For zero orifice yaw, the flow structure downstream of the synthetic jet is similar to that observed for a steady jet in crossflow. Here, the momentum impulse from the formation phase of the synthetic jet gives rise to a weak counter-rotating vortex pair.[11] At this velocity ratio, the vortex pair is centered near the boundary-layer edge and would likely provide little assistance in boundary-layer separation control. For nonzero yaw angles, it appears that an increase in orifice yaw angle has two effects on the jet–boundary-layer interaction. First, orifice yaw distorts the jet formation vortex on the upstream side of the orifice leading to a turning of the forming jet toward the downstream edge; second, the increased projected area of the jet leads to a greater downstream deflection by the incoming flow. For $\beta = 10$ deg, these two effects combine to create sufficient cross-stream and spanwise momenta to lead to the formation of a single streamwise vortex similar in character to the streamwise vortex created by a vortex generator jet (see, for example, Refs. 3 and 17). For $\beta = 20$ deg, these effects lead to a rapid and acute downstream turning of the jet with the result that the jet functions primarily as a fluid obstacle in the boundary layer with a rapidly closing wake and a horseshoe vortex whose legs help to mix high-momentum fluid into the lee of the actuator.

With respect to the second of the two effects due to yaw, a simple alternative interpretation of this effect is that changing the yaw angle of the orifice changes the apparent spanwise scale of the jet. A simplified control volume analysis of a synthetic jet in a crossflow boundary layer shows that, for a constant velocity ratio, the angular deflection of the jet should vary as

$$\tan\alpha \sim (w/L)^{-1}(h/\delta)$$

where α is the angle of the deflected jet measured relative to the horizontal, w is the jet width at the orifice, and δ is a boundary-layer length scale, not necessarily equal to the boundary-layer thickness. We note that w/L increases from 0.01 at $\beta = 0$ deg to 0.17 at $\beta = 10$ deg and finally to 0.34 at $\beta = 20$ deg. This alternative interpretation provides some useful perspective for understanding

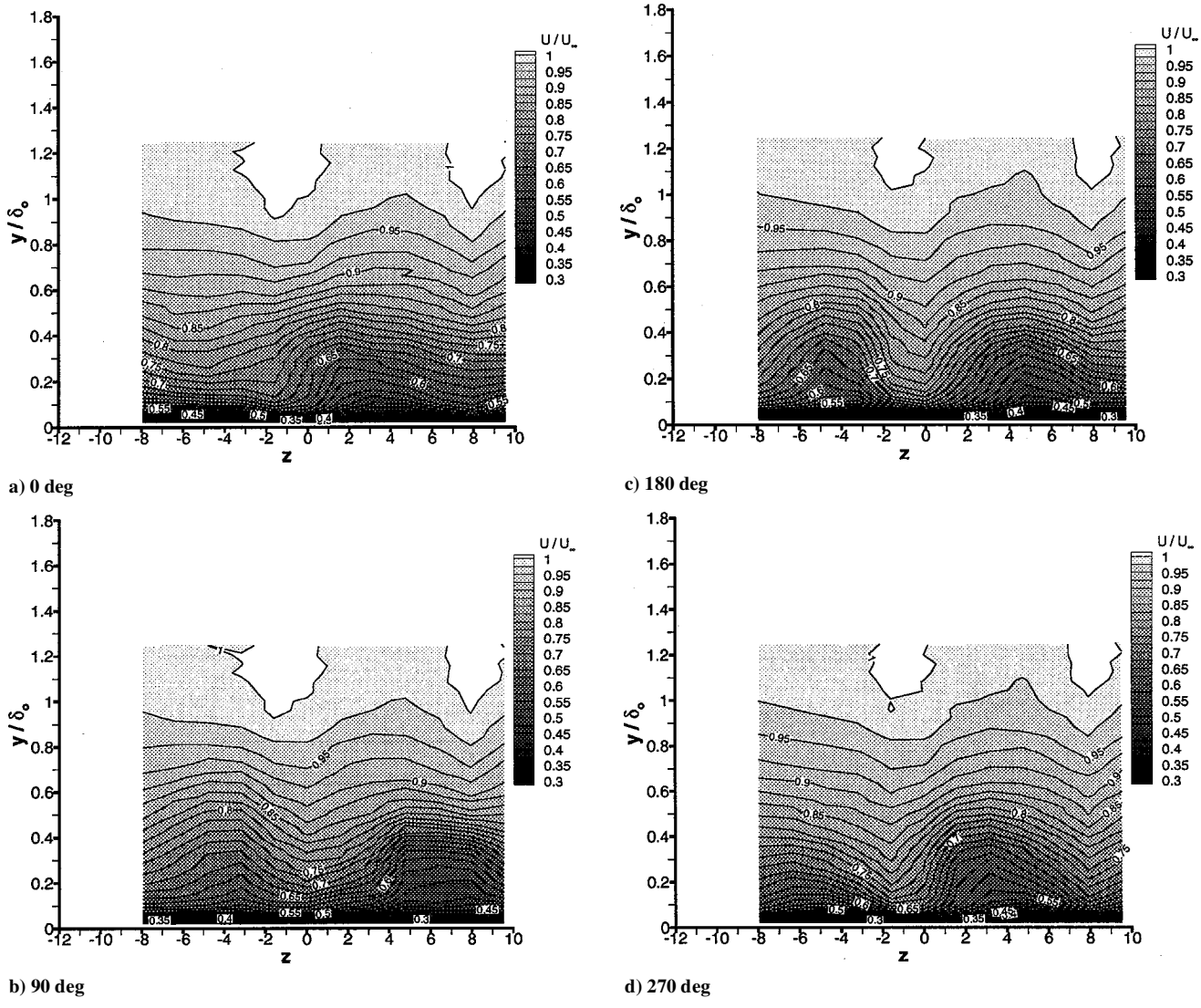

Fig. 10 Phase-averaged contours of the mean streamwise velocity for β = 20 deg at x/L = 1.0.

the effect of orifice yaw on the change in the flowfield. Although the magnitude of the change in the yaw angle appears modest, the relative spanwise scale of the jet changes by a factor of 34, and the deflection of the jet changes notably as indicated in the results shown. Finally, we can also conclude from this simple analysis that a wider orifice (h), relative to the boundary-layer thickness, would be expected to increase the range of β values for which a single vortex is formed in a synthetic jet–boundary-layer interaction.

IV. Conclusions

The mean flow features in the boundary layer downstream of a wall-mounted synthetic jet were studied for three yaw orientations of a rectangular synthetic jet. When the orifice was aligned with the mean freestream velocity ($\beta = 0$ deg), a flow structure consistent with a weak counter-rotating vortex pair was observed in the boundary layer. This structure was established within one orifice length downstream of the actuator center and appeared to be a steady feature of the flow but with an amplitude and position in the boundary layer that varied at the actuator driver frequency. For $\beta = 10$ deg, contours of mean streamwise velocity across the span of the interaction suggested the presence of a single vortex in the boundary layer. Looking downstream, the vortex had a counterclockwise rotation, sweeping high-momentum fluid toward the wall for $z < 0$ and pushing low-momentum fluid up in the boundary layer for $z > 0$. For $\beta = 20$ deg, a flow structure more closely resembling a horseshoe vortex appeared. For all three yaw angles, the observed flow structures were modulated at the driving frequency of the actuator indicating a persistent unsteadiness in the near field of the interactions. Also for all three yaw angles, elevated streamwise turbulence intensity levels were observed in the boundary layer, and cross-span contours of this quantity resembled in shape the contours of the mean streamwise velocity.

Acknowledgments

This work was supported through a grant from NASA Langley Research Center (NAG-1-01063), monitored by Frank Chen.

References

[1] Johnston, J. P., and Nishi, M., "Vortex Generator Jets—Means for Flow Separation Control," *AIAA Journal*, Vol. 28, No. 6, 1990, pp. 989–994.

[2] Compton, D. A., and Johnston, J. P., "Streamwise Vortex Production by Pitched and Skewed Jets in a Turbulent Boundary Layer," *AIAA Journal*, Vol. 30, No. 3, 1992, pp. 640–647.

[3] Zhang, X., and Collins, M. W., "Measurements of a Longitudinal Vortex Generated by a Rectangular Jet in a Turbulent Boundary Layer," *Physics of Fluids*, Vol. 9, No. 6, 1997, pp. 1665–1673.

[4] Seifert, A., Bachar, T., Koss, D., Shepshelovich, M., and Wygnanski, I., "Oscillatory Blowing: A Tool to Delay Boundary-Layer Separation," *AIAA Journal*, Vol. 31, No. 11, 1993, pp. 2052–2060.

[5] Amitay, M., and Smith, B. L., and Glezer, A., "Aerodynamic Flow Control Using Synthetic Jet Technology," AIAA Paper 98-0208, Jan. 1998.

[6] Amitay, M., Smith, D. R., and Kibens, V., Parekh, D. E., and Glezer, A., "Aerodynamic Flow Control over an Unconventional Airfoil Using Synthetic Jet Actuators," *AIAA Journal*, Vol. 39, No. 3, 2001, pp. 361–370.

[7]Amitay, M., Pitt, D., and Glezer, A., "Separation Control in Duct Flows," *Journal of Aircraft*, Vol. 39, No. 4, 2002, pp. 616–620.

[8]Rinehart, C., and Glezer, A., "Synthetic Jet-Based Vortex Generation for Aerodynamic Flow Control," American Physical Society, Paper AF7, Nov. 1999.

[9]Smith, D. R., "The Interaction of a Synthetic Jet with a Cross-Flow Boundary Layer," *AIAA Journal*, Vol. 40, No. 11, 2002, pp. 2277–2288.

[10]Weston, R. P., and Thames, F. C., "Properties of Aspect-Ratio-4.0 Rectangular Jets in a Subsonic Crossflow," *Journal of Aircraft*, Vol. 16, No. 10, 1979, pp. 701–707.

[11]Broadwell, J. E., and Breidenthal, R. E., "Structure and Mixing of a Transverse Jet in incompressible Flow," *Journal of Fluid Mechanics*, Vol. 148, 1984, pp. 405–412.

[12]Eroglu, A., and Breidenthal, R. E., "Structure, Penetration, and Mixing of Pulsed Jets in Crossflow," *AIAA Journal*, Vol. 39, No. 3, 2001, pp. 417–423.

[13]Chang, Y. K., and Vakili, A. D., "Dynamics of Vortex Rings in Crossflow," *Physics of Fluids*, Vol. 7, No. 7, 1995, pp. 1583–1597.

[14]Johari, H., Pacheco-Tougas, M., and Hermanson, J. C., "Penetration and Mixing of Fully Modulated Turbulent Jets in Crossflow," *AIAA Journal*, Vol. 37, No. 7, 1999, pp. 842–850.

[15]Smith, B. L., and Glezer, A., "The Formation and Evolution of Synthetic Jets," *Physics of Fluids*, Vol. 10, No. 9, 1998, pp. 2281–2297.

[16]Shabaka, I. M. M. A., Mehta, R. D., and Bradshaw, P., "Longitudinal Vortices Imbedded in Turbulent Boundary Layers. Part 1. Single Vortex," *Journal of Fluid Mechanics*, Vol. 155, 1985, pp. 37–57.

[17]Khan, Z. U., and Johnston, J. P., "On Vortex Generating Jets," *International Journal of Heat and Fluid Flow*, Vol. 21, 2000, pp. 506–511.

[18]Smith, B. L., Trautman, M. A., and Glezer, A., "Controlled Interactions of Adjacent Synthetic Jet Actuators," AIAA Paper 99-0669, Jan. 1999.

W. J. Dahm
Associate Editor